J. Am. Chem. Soc. **1986**, *108*, 7010–7016

# Bis($\eta^6$-hexamethylbenzene)($\eta^4$,$\eta^6$-[$2_4$](1,2,4,5)cyclophane)diruthenium(0,II) Bis(tetrafluoroborate). A Novel Mixed-Valence Ion (Class II) Exhibiting a Net Two-Electron Intervalence Transfer

**Richard H. Voegeli, Hee Chol Kang, Richard G. Finke,* and V. Boekelheide***

*Contribution from the Department of Chemistry, University of Oregon, Eugene, Oregon 97403.*

*Received March 28, 1986*

**Abstract:** Syntheses of bis($\eta^6$-hexamethylbenzene)($\eta^4$,$\eta^6$-[$2_4$](1,2,4,5)cyclophane)diruthenium(0,II) bis(tetrafluoroborate) (**3**) by chemical (electron reservoir) and electrochemical reduction of bis($\eta^6$-hexamethylbenzene)($\eta^6$,$\eta^6$-[$2_4$](1,2,4,5)-cyclophane)diruthenium(II,II) tetrakis(tetrafluoroborate) (**2**) are described. A further two-electron reduction of **3** gives the neutral diruthenium(0,0) species **4**. Cyclic voltammetry and coulometry of **2** show a reversible, *net*, two-electron reduction wave ($E_{1/2}$(SCE) = −0.060 ± 0.005 V) giving **3** and, in turn, a second reversible, *net*, two-electron wave ($E_{1/2}'$(SCE) = −0.593 ± 0.005 V) converting **3** to **4**. The comproportionation constant ($K_c$) for the equilibrium [$\mathbf{2} + \mathbf{4} \rightleftharpoons 2\,\mathbf{3}$] is $1.07 \times 10^{18}$. A variable-temperature $^1$H NMR study shows **3** to be a fluxional molecule (**3a** $\rightleftharpoons$ **3b**) with an energy barrier ($\Delta H^{\ddagger}$) for conformational interconversion of 12.7 ± 0.8 kcal/mol. An intervalence transfer band for **3**, measured in dichloromethane, exhibits a maximum, $E_{op}$, at 19 800 ± 100 cm$^{-1}$ (56.5 ± 0.3 kcal/mol) and an extinction coefficient of 485. The novel feature of **3** is that it is the first discrete, nonpolymeric, mixed valence ion class II exhibiting a *net* two-electron intervalence transfer; furthermore, both the thermal and optical barriers for **3** have been measured. Possible ways of rationalizing the properties of **3** with respect to current theory are discussed.

The outstanding characteristic of [$2_n$]cyclophanes is the delocalization of their $\pi$-electron systems.[1-4] This, combined with the possibility for metal complexation at both outside faces of the arene decks of a [$2_n$]cyclophane, has raised the question of whether suitable polymers of transition-metal complexes of [$2_n$]cyclophanes, as depicted by **1**,[5] might show complete $\pi$-electron delocalization over the whole of the polymer molecule and, possibly, so lead to electrical conductivity. To gain insight regarding the potential properties of such polymers we have prepared **2**, as a model subunit related to **1**, and have converted **2**, as shown in Scheme I, to the partially reduced species **3** and to the fully reduced neutral compound **4**. We now describe the details of these preparations and the unusual properties of the mixed-valence ion **3**.

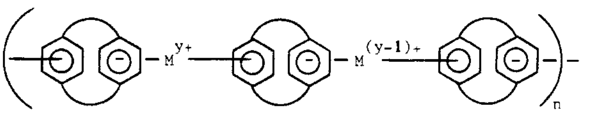

1

A requirement for an electrically conducting polymer such as **1** is that it have a conduction band, and this, in turn, requires that a subunit of the polymer, such as **3**, have mixed-valence properties. Ruthenium was chosen as the transition metal for our model subunit on the basis of our earlier studies on the syntheses of metal complexes of [$2_n$]cyclophanes,[6-8] and our choice of [$2_4$](1,2,4,5)cyclophane arose out of our studies on the electrochemical behavior of a series of ruthenium complexes of [$2_n$]cyclophanes.[8,9]

Scheme I

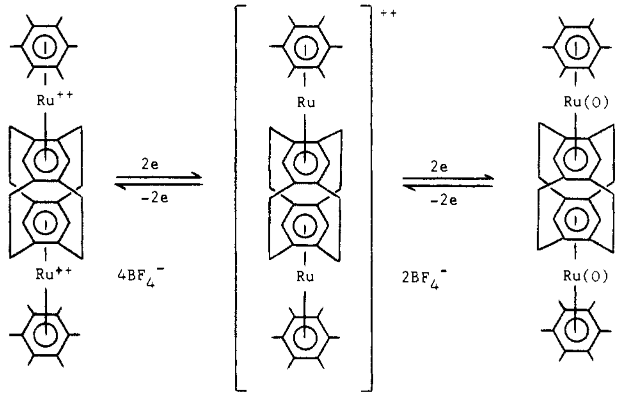

2 3 4

The formation of **2** by the reaction of ($\eta^6$-hexamethylbenzene)ruthenium(II) tris(acetone) solvate, **5**, with [$2_4$](1,2,4,5)cyclophane (**6**) was carried out as previously described.[8] The reduction of **2**, as shown in Scheme I, can be accomplished either electrochemically or chemically. Both reduction steps are completely reversible. However, preparative isolation of **3** from bulk electrolysis of **2** is not feasible because of the difficulty of separating **3** from the supporting electrolyte. Since **4** is soluble in benzene, it can be readily removed from the electrolyte after bulk electrolysis of **2** and is conveniently prepared in this way in 92% yield. Chemical reduction of **2** with sodium amalgam to give **4** is also successful, but only in 34% yield.

The method of choice for the preparative reduction of **2**, to either **3** or **4**, is to use an "electron reservoir" compound of the type given prominence by Astruc.[10,11] For our purposes, instead

---

[1] Kovac, B.; Mohray, M.; Heilbronner, E.; Boekelheide, V.; Hopf, H. *J. Am. Chem. Soc.* **1980**, *102*, 4314–4324.

[2] Heilbronner, E.; Yang, Z.-z. *Top. Curr. Chem.* **1983**, *115*, 1–55.

[3] Gerson, F. *Top. Curr. Chem.* **1984**, *115*, 57–105.

[4] For [$2_n$]cyclophane nomenclature, see: Boekelheide, V. *Top. Curr. Chem.* **1983**, *113*, 87–143. Preliminary publication of certain aspects of this manuscript is in the following: Boekelheide, V. *Pure Appl. Chem.* **1986**, *58*, 1–6.

[5] The following is a generalized structure representing any one of the possible [$2_n$]cyclophanes:

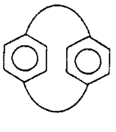

[6] Laganis, E. D.; Finke, R. G.; Boekelheide, V. *Tetrahedron Lett.* **1980**, *21*, 4405–4408.

[7] Laganis, E. D.; Finke, R. G.; Boekelheide, V. *Proc. Natl. Acad. Sci. U.S.A.* **1981**, *78*, 2657–2658.

[8] Laganis, E. D.; Voegeli, R. H.; Swann, R. T.; Finke, R. G.; Hopf, H.; Boekelheide, V. *Organometallics* **1982**, *1*, 1415–1420.

[9] Finke, R. G.; Voegeli, R. H.; Laganis, E. D.; Boekelheide, V. *Organometallics* **1983**, *2*, 347–350 and references therein.

0002-7863/86/1508-7010\$01.50/0

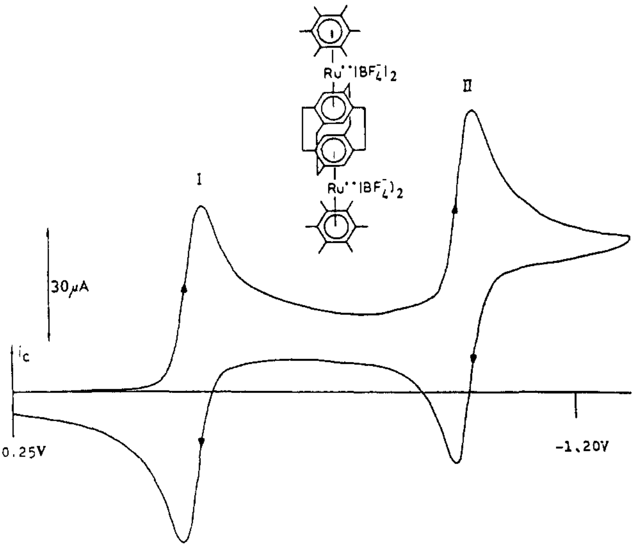

**Figure 1.** Cyclic voltammogram of **2** in acetone measured at room temperature at 100 mV/s. $E_{1/2}^{\mathrm{I}}$(SCE) = −0.060 ± 0.005 V and $E_{1/2}^{\mathrm{II}}$(SCE) = −0.593 ± 0.005 V.

of a 19-electron iron complex, we chose the readily available 20-electron complex, bis($\eta^4$,$\eta^6$-hexamethylbenzene)ruthenium(0) (**8**).[12] When 2 equiv of **8** were employed in the reaction with **2**, using methanol as solvent, the neutral ruthenium(0) derivative **4** was isolated in a very pure state and in high yield. When only 1 equiv of **8** was employed, formation of the mixed-valence ion **3** occurred in quantitative yield. Fortuitously, **3** is readily soluble in dichloromethane and so can be easily separated by extraction from the accompanying, insoluble side product, bis($\eta^6$-hexamethylbenzene)ruthenium(II) bis(tetrafluoroborate) (**9**). This is an interesting example of the usefulness of **8** as an "electron reservoir" compound.

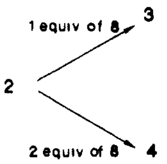

In accord with the bulk electrolysis experiments, the cyclic voltammogram of **2**, as shown in Figure 1, was measured in acetone at room temperature with tetra-*n*-butylammonium tetrafluoroborate as electrolyte and with a scan rate ($\nu$) of 100 mV/s. It showed two completely reversible, two-electron waves: $E_{1/2}$(SCE) = −0.060 ± 0.005 V, $\Delta E_p$ = 35 ± 3 mV, $i_a/i_c$ = 1.00 ± 0.01; $E_{1/2}'$(SCE) = −0.593 ± 0.005 V, $\Delta E_p$ = 36 ± 3 mV, $i_a/i_c$ = 0.95 ± 0.05. The $\Delta E_p$ values indicated that a net two-electron transfer ("direct" two-electron transfer)[9] was occurring for each wave, and this was confirmed by coulometry. Thus, the overall process for the electrolytic reduction of **2** is in accord with that given in Scheme I.

The relationship of the concentrations of **2**, **4**, and **3** at equilibrium (eq 1) is given by the comproportionation constant, $K_c$.

$$\mathbf{2} + \mathbf{4} \xrightleftharpoons{K_c} 2\,\mathbf{3} \qquad (1)$$

The value of $K_c$ can be deduced from the cyclic voltammetry data by using the easily derived eq 2.[13] Employing this equation with $(E_1^0 - E_2^0)$ = 533 mV and $n_1 = n_2 = 2$, we find the comproportionation constant, $K_c$ (298 K), for eq 1, to be $1.07 \times 10^{18}$.

$$K_c = \exp\left[\frac{(n_1E_1^0 - n_2E_2^0)F}{RT}\right] \qquad (2)$$

The reaction given by eq 1 can also be used as a means of preparing **3**. When a pale yellow solution of **2** is added to a solution containing an equimolar quantity of the golden yellow **4**, dark red crystals of the mixed-valence ion **3** are formed. After isolation and recrystallization from either methanol or dichloromethane, **3** forms purplish-red needles having a metallic sheen. In view of the large value of the comproportionation constant, $K_c$, solutions of **3** can be treated as containing essentially pure **3**.

It was of high interest to examine the properties of **3** to see how they might relate to current theories of intervalence electron transfer. Undoubtedly, the most famous and best studied mixed-valence ion is the ruthenium–pyrazine complex

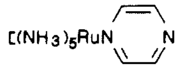

first described by Creutz and Taube in 1969.[14,15] The properties of the Creutz–Taube ion have stimulated an unprecedented amount of work on the theory and interpretation of electron transfer in mixed-valence ions. It was against this background of the extensive work on the Creutz–Taube ion and the development of the theory of electron transfer by Hush[17-19] and by others[20-23] that we examined the properties of **3**. Although a complete description of the Creutz–Taube ion remains unsettled,[16] numerous other mixed-valence ions of the ruthenium ammine type have been prepared and classified as being localized[13,20,24-28] or delocalized (valence averaged) systems.[23,29,30]

At room temperature the $^1$H and $^{13}$C NMR spectra ($CD_2Cl_2$) of **3** show the molecule to be symmetrical. The methyl protons of the two hexamethylbenzene rings of **3** appear as a singlet at $\delta$ 2.17. Likewise, its proton-decoupled $^{13}$C NMR spectrum shows the methyl carbons of the two hexamethylbenzene rings as a singlet at $\delta$ 17.4 and the cyclophane–aromatic C–H carbons as a singlet at $\delta$ 77.2. Thus, on the NMR time scale at room temperature, the symmetry of the spectra of **3** suggests the presence of a $Ru^+$–$Ru^+$ system. However, when the measurements are made at lower temperatures, the NMR signals broaden, coalesce, and eventually separate into two sets of signals, *indicating two localized $\pi$–d electron systems and two conformations separated by a measurable energy barrier.* This is consistent with the assignment of localized $Ru^{2+}$–$Ru^0$ sites at lower temperatures. In Figure 2, the results of a variable-temperature study of the $^1$H NMR spectrum of **3** are summarized. The signal for the methyl protons of the two hexamethylbenzene rings of **3** was measured at eight

---

(10) Astruc, D.; Hamon, J.-R.; Althoff, G.; Roman, E.; Batail, P.; Michaud, P.; Mariot, J. P.; Varret, F.; Cozak, D. *J. Am. Chem. Soc.* **1979**, *101*, 5445–5447.

(11) Hamon, J.-R.; Astruc, D.; Michaud, P. *J. Am. Chem. Soc.* **1981**, *103*, 758–766, and subsequent papers.

(12) We thank the late Professor E. L. Muetterties for his kindness in providing us with the preparation of **8**. The procedure is given now in detail in ref 36.

(13) (a) $K_c$ has not been corrected for the statistical factor of 4.[13b,c] (b) Richardson, D. E.; Taube, H. *Inorg. Chem.* **1981**, *20*, 1278–1285. (c) Richardson, D. E.; Taube, H. *J. Am. Chem. Soc.* **1983**, *105*, 40–51.

(14) Creutz, C.; Taube, H. *J. Am. Chem. Soc.* **1969**, *91*, 3988–3989.

(15) Creutz, C.; Taube, H. *J. Am. Chem. Soc.* **1973**, *95*, 1086–1094.

(16) Fürholz, U.; Bürgi, H.-B.; Wagner, F. E.; Stebler, A.; Ammeter, J. H.; Krausz, E.; Clark, R. J. H.; Stead, M. J.; Ludi, A. *J. Am. Chem. Soc.* **1984**, *106*, 121–123.

(17) Allen, G. C.; Hush, N. S. *Prog. Inorg. Chem.* **1967**, *8*, 357–391.

(18) Hush, N. S. *Prog. Inorg. Chem.* **1967**, *8*, 391–444.

(19) Hush, N. S. *Electrochim. Acta* **1968**, *13*, 1005–1023.

(20) Sutton, J. E.; Sutton, P. M.; Taube, H. *Inorg. Chem.* **1979**, *18*, 1017–1021.

(21) Wong, K. Y.; Schatz, P. N. *Prog. Inorg. Chem.* **1981**, *28*, 369–449.

(22) Meyer, T. J. *Acc. Chem. Res.* **1978**, *11*, 94–100.

(23) Cannon, R. *Electron Transfer Reactions*; Butterworths: London, 1980; pp 175–220.

(24) Sutton, J. E.; Taube, H. *Inorg. Chem.* **1981**, *20*, 3125–3134.

(25) Stein, C. A.; Taube, H. *J. Am. Chem. Soc.* **1981**, *103*, 693–695.

(26) Stein, C. A.; Taube, H. *J. Am. Chem. Soc.* **1978**, *100*, 1635–1637.

(27) Tanner, M.; Ludi, A. *Inorg. Chem.* **1981**, *20*, 2348–2350.

(28) Tom, G. M.; Creutz, C.; Taube, H. *J. Am. Chem. Soc.* **1974**, *96*, 7827–7829.

(29) Tom, G. M.; Taube, H. *J. Am. Chem. Soc.* **1975**, *97*, 5310–5311.

(30) Krentzien, H.; Taube, H. *J. Am. Chem. Soc.* **1976**, *98*, 6379–6380.

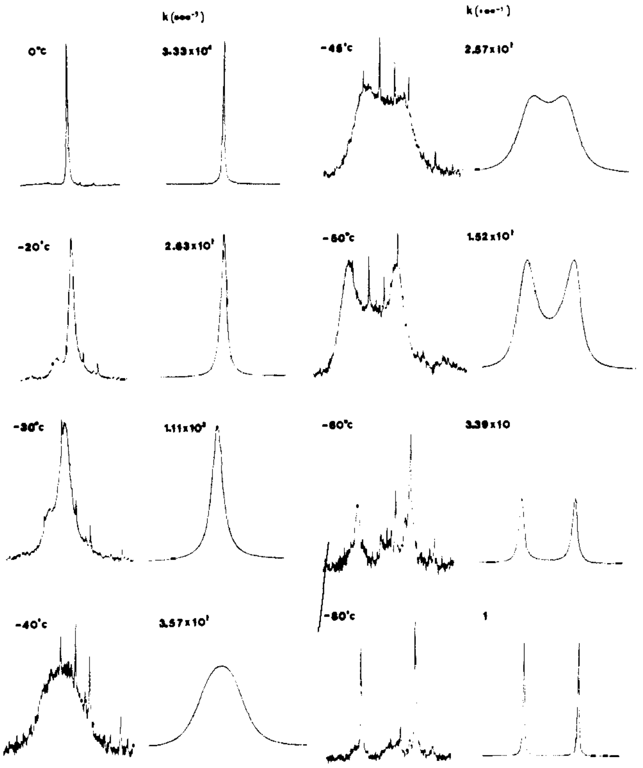

**Figure 2.** $^1$H NMR spectra of **3** measured in $CD_2Cl_2$ over a series of eight temperatures ranging from 0 to −80 °C and compared with their corresponding computer-simulated spectra at each of these temperatures. The rates of conformational change were deduced by using the GNTXCH program of the Nicolet 360-MHz spectrometer. The signal, whose coalescence and splitting is being observed, is that of the methyl protons present in the hexamethylbenzene decks. As the signal broadens, it overlaps signals due to the bridging methylene protons, which produces the spikes observed in the experimental spectrum.

different temperatures, ranging from 0 to −80 °C. As shown, this signal is a sharp singlet down to −20 °C; it then broadens, coalescing at −43 °C; and at −60 °C and lower it appears as two fairly sharp singlets. Applying the computer simulation program (GNTXCH) of the Nicolet 360-MHz spectrometer to these data, we were able to measure the rates for the thermal intervalence transfer for **3** at these various temperatures, and these simulations and rate values are included in Figure 2. The fact that the observed rates did not change with a sixfold change in concentration demonstrates that the thermal electron transfer is an intramolecular and not an intermolecular process.

The rate process was analyzed by using the Eyring rate equation and, from a plot of log ($k/T$) vs. $1/T$, we were able to obtain the activation parameters, $\Delta H^\ddagger$ and $\Delta S^\ddagger$. The observed plot, shown in Figure 3, exhibits excellent linearity (correlation coefficient = 0.997). The data on which Figure 3 is based are given in the Experimental Section. From the slope (2760 ± 160) and intercept (12.10 ± 0.65) terms from Figure 3, the values for the kinetic parameters for the thermal conformational equilibrium of **3** are $\Delta H^\ddagger = 12.7 \pm 0.8$ kcal/mol; $\Delta S^\ddagger = 8 \pm 3$ cal/(mol K); and $\Delta G_{298K} = 10.3 \pm 1.2$ kcal/mol.

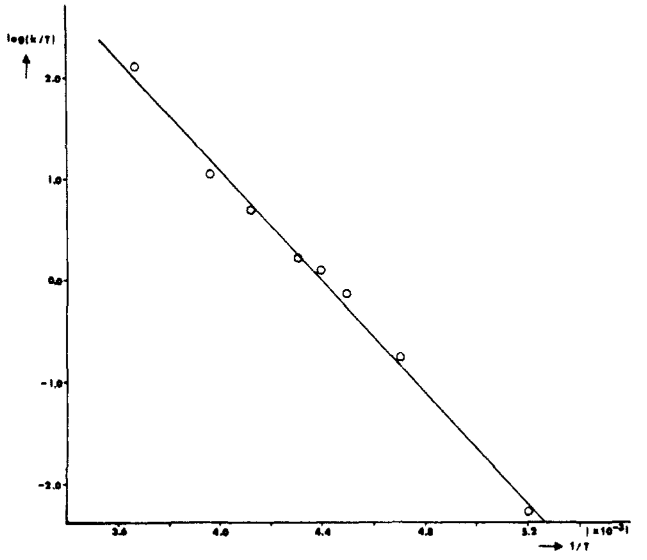

**Figure 3.** Determination of the kinetic parameters for the conformational fluctuation of **3** by a plot of log ($k/T$) vs. $1/T$. Observed slope = 2760 ± 160 and the intercept = 12.10 ± 0.65.

It is well-known that the reduction of the planar bis($\eta^6$-hexamethylbenzene)ruthenium(II) ion gives bis(hexamethylbenzene)ruthenium(0), **8**, as a fluxional molecule.[31-33] Its structure, deduced from $^1$H NMR data and from X-ray analysis, has a bent, boat-shaped arene ring, as shown by **8**.[34] This change in geometry of arene–ruthenium complexes, when ruthenium undergoes a change in oxidation state from (II) to (0), has been shown to be the controlling factor influencing the electrode potential required for two-electron reductions of arene–ruthenium(II)–[2$_n$]cyclophane complexes.[8,9] If the [2$_n$]cyclophane is rigid and cannot readily deform to accommodate a change from $\eta^6$- to $\eta^4$-bonding, it is then the arene that deforms from planarity. However, if the [2$_n$]cyclophane is quite flexible, or has benzene decks that are naturally boat-shaped in the free hydrocarbon, it is the [2$_n$]cyclophane that adopts to $\eta^4$-bonding to the ruthenium(0) atom. From an X-ray crystallographic study, free [2$_4$](1,2,4,5)cyclophane is known to have boat-shaped benzene decks.[35] Furthermore, the reduction of **10** to **11** has been examined by both $^1$H and $^{13}$C NMR studies, and it is clear that the hexamethylbenzene ring retains its $\eta^6$-bonding during the reduction process, whereas the [2$_4$](1,2,4,5)cyclophane moiety changes from being bound $\eta^6$ in **10** to being bound $\eta^4$ in **11**.[36]

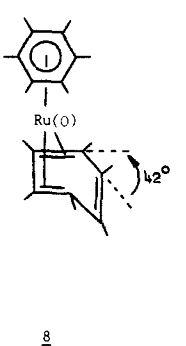

8

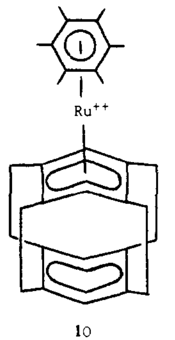

10

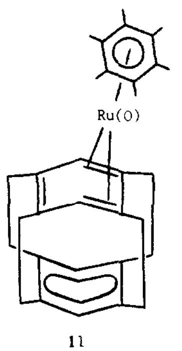

11

The methyl protons of the hexamethylbenzene deck appear as a singlet at δ 2.32 ($CD_3COCD_3$) in the $^1$H NMR spectrum of **10**. On reduction of **10** to **11**, the signal for these same methyl protons shifts upfield to δ 1.92 ($C_6D_6$). By comparison the methyl protons of the hexamethylbenzene decks of **3** at 25 °C appear as a singlet at δ 2.17 ($CD_2Cl_2$), but then split into two different singlets at −80 °C, appearing at δ 2.36 and 1.87. Even though of necessity the solvents used in this comparison are different, it is still quite evident that the two different environments experienced by the methyl protons of the two hexamethylbenzene decks of **3** are closely similar to the two environments present in the model compounds **10** and **11**. On the basis of this comparison, the simplest and most reasonable interpretation of the variable-temperature studies of **3** is that the dynamic equilibrium being ob-

---

[31] Fischer, E. O.; Elschenbroich, Ch. *Chem. Ber.* **1970**, *103*, 162–172.

[32] Darensbourg, M. Y.; Muetterties, E. L. *J. Am. Chem. Soc.* **1978**, *100*, 7425–7428.

[33] Muetterties, E. L.; Bleeke, J. R. *Acc. Chem. Res.* **1979**, *12*, 324–330.

[34] Huttner, G.; Lange, S. *Acta Crystallogr.* **1972**, *B28*, 2049–2060.

[35] Hanson, A. W. *Acta Crystallogr. Sect. B* **1977**, *33*, 2003–2007.

[36] Swann, R. T.; Hanson, A. W.; Boekelheide, V. *J. Am. Chem. Soc.* **1986**, *108*, 3324–3334.

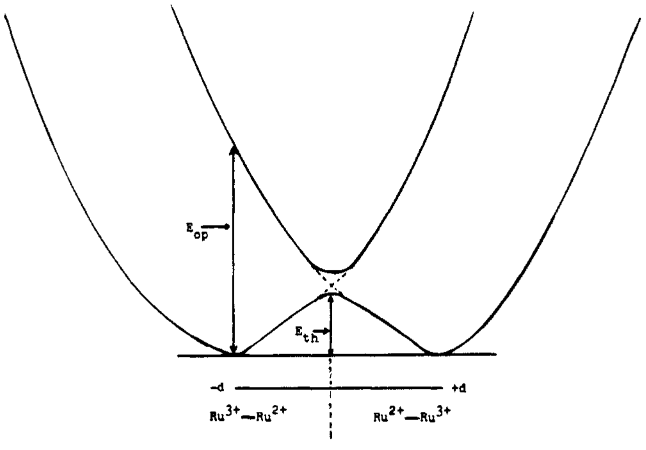

**Figure 4.** Diagram of potential energy vs. nuclear configuration in a two-state description of the mixed-valence ion of a typical diruthenium-ammine complex.

served is one involving a *net* two-electron transfer as shown below by the equilibrium between **3a** and **3b**.

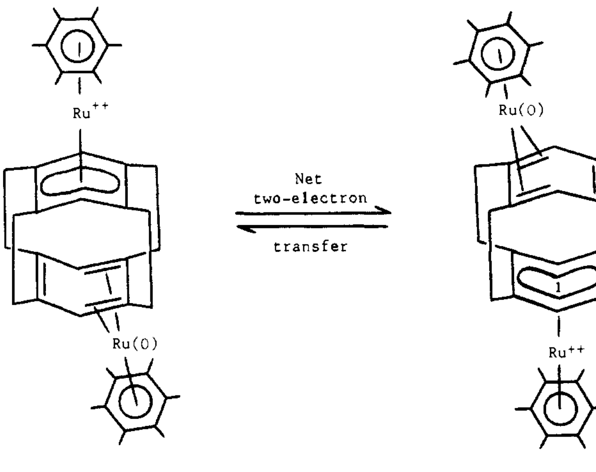

3a 3b

The conclusion that **3** is a mixed-valence ion class II, containing two different types of ruthenium atoms, is also consistent with an X-ray photoelectron spectral analysis. This analysis of **3** showed two signals at 280.8 and 282.0 eV, indicating two types of ruthenium atoms. However, the validity of this experiment suffers from the same considerations pointed out in a recent reassessment of the X-ray photoemission behavior of the Creutz–Taube ion.[37]

A crucial point is whether or not the *net* two-electron transfer, **3a** ⇌ **3b**, proceeds via stepwise single-electron transfers. In our electrochemical studies of the reduction of **8** and of arene–ruthenium(II)–[$2_n$]cyclophanes such as **10**, we were able to show that the *net* two-electron waves, observed by cyclic voltammetry in acetone, either broadened or separated into two one-electron waves in less polar solvents.[8,9] This provided good evidence that the general reduction process in **8** and **10** consists of two discrete, one-electron steps. These studies suggest that for complex **10** the important energy barrier is that required to change the geometry of the complex to allow the first electron to be transferred. Transfer of the second electron then occurs with little additional energy barrier. Unfortunately, in the case of **3**, a similar analysis of the change of the cyclic voltammogram in solvents less polar than acetone could not be made due to solubility difficulties and electrode adsorption phenomena. However, although not proven, it would seem likely that the reduction of **3**, just as for **10**, occurs by two discrete, one-electron steps and, quite probably, the thermal electron-transfer involved in the equilibrium **3a** ⇌ **3b** proceeds in a similar manner. Thus, the value of $\Delta H^{\ddagger} = 12.7 \pm 0.8$ kcal/mol, found for **3** from our variable-temperature NMR studies, probably corresponds to the barrier for a single-electron transfer and so to the $E_{th}$ value in the usual potential energy diagram,[18] such as that given in Figure 4 (or more precisely Figure 6, vide infra).

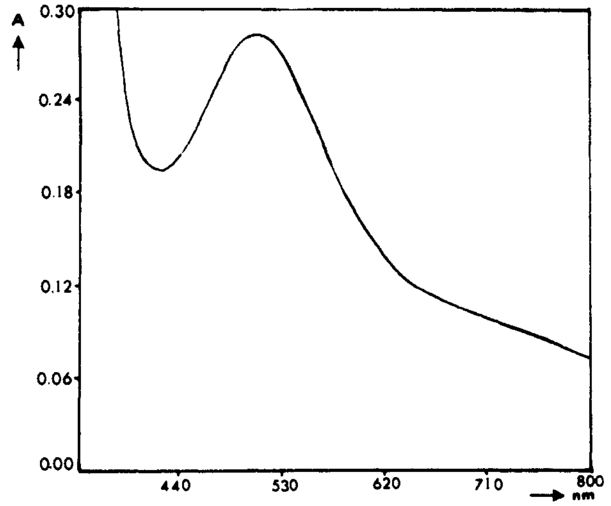

**Figure 5.** Plot of absorbance vs. wavelength for the intervalence transfer band of **3** measured in dichloromethane at room temperature. Compounds **2** and **4** have no appreciable absorption beyond 440 nm.

One-electron, mixed-valence systems of the ruthenium–ammine type show a characteristic absorption band in the visible to near infrared region that is commonly called the intervalence charge-transfer band.[38–40] This band is assigned to the vertical Franck–Condon transition, $E_{op}$ in Figure 4, although the deficiencies of the Franck–Condon and Born–Oppenheimer approximations and the inadequacy of the representation as a vertical transition between single potential surfaces for significantly delocalized systems have been noted.[21]

The absorption spectrum of **3**, measured in dichloromethane and presented in Figure 5, has a maximum ($\nu$) at 19 800 ± 100 $cm^{-1}$ (56.5 ± 0.3 kcal/mol), a molar extinction coefficient ($\epsilon_{max}$) of 485 ± 27 $M^{-1}$ $cm^{-1}$, and a width at half-height ($\Delta\nu_{1/2}$) of 9000 ± 200 $cm^{-1}$. Neither the fully oxidized species, **2**, nor the fully reduced species, **4**, shows any absorption in this region. Also, a search in the region of 800–1900 nm showed no additional absorption for the mixed-valence ion **3**.

It would be desirable to construct a potential energy diagram for **3** which would allow an assignment and interpretation of the measured values, $E_{op}$ and $E_{th}$. However, the usual one-electron intervalence transfer diagrams given for the ruthenium–ammine systems, such as Figure 4, are not adequate for this purpose, since we are confronted with interconnecting, two-electron ground states in the case of **3**. To adapt Figure 4 to the case of **3** by simply having two-electron potential wells would predict $E_{op}$ to be a two-electron process, $Ru^{2+}$–$Ru^0$ + $h\nu$ → *$Ru^0$–$Ru^{2+}$. The oscillator strength for such a formally forbidden process should be quite low, whereas the absorption band for **3** is reasonably strong.

Precedent for the treatment of two-electron transfers is available, though, from the theoretical and spectroscopic studies of the polymeric halides of Pt(II)/Pt(IV)[43] and Sb(III)/Sb(V).[44]

---

(37) Citrin, P. H.; Ginsberg, A. P. *J. Am. Chem. Soc.* **1981**, *103*, 3673–3679.

(38) Felix, F.; Ludi, A. *Inorg. Chem.* **1978**, *17*, 1782–1785.

(39) Powers, M. J.; Meyers, T. J. *Inorg. Chem.* **1978**, *17*, 1785–1790.

(40) Taube, H. *Ann. New York Acad. Sci.* **1978**, *313*, 481–495.

(41) Since X-ray crystallographic data are not available for **3**, the internuclear distance (*r*) between the ruthenium atoms has been estimated to be 6.22 ± 0.05 Å, based on the average distance (2.69 ± 0.03 Å) between decks of [$2_4$](1,2,4,5)cyclophane[35] and the ruthenium-to-cyclophane deck distance (1.76 ± 0.05 Å, based on an estimate of the average for Ru(II) and Ru(0)) for ($\eta^6$-hexamethylbenzene)($\eta^6$-4,12-dimethyl-7,15-dimethoxy[$2_2$](1,3)-cyclophane)ruthenium(II) bis(tetrafluoroborate)).[42]

(42) Hanson, A. W. *Cryst. Struct. Commun.* **1982**, *11*, 1019–1026.

(43) Clark, R. J. H. *Chem. Soc. Rev.* **1984**, *13*, 219–244.

(44) Prassides, K.; Day, P. *J. Chem. Soc., Faraday Trans. 2* **1984**, *80*, 85–95.

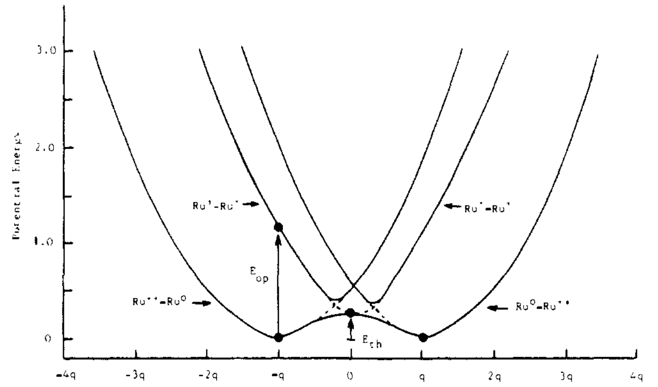

Figure 6. Potential energy diagram for the mixed-valence ion **3**. The ratio of $E_{op}/E_{th}$ is shown approximately to scale of the observed ratio of 56.5/12.7 = 4.4. The four solid circles (●) indicate the experimentally determined points of this diagram. The dashed lines near $q = 0$ show the connectivity of the original three curves ($Ru^{2+}$–$Ru^0$, $Ru^0$–$Ru^{2+}$, and $Ru^+$–$Ru^+$) and, hence, the avoided curve crossings.

For these examples, diagrams have been devised having three harmonic potential wells. For the case of the antimony halides, the potential wells are one each for $Sb^{III}$–$Sb^{V}$, $Sb^{V}$–$Sb^{III}$, and $Sb^{IV}$–$Sb^{IV}$. $E_{op}$ is thus assigned to the one-electron transition, $Sb^{III}$–$Sb^{V} + h\nu \rightarrow Sb^{IV}$–$Sb^{IV}$. A similar analysis made for the platinum halides is well-supported by resonance Raman data.[43] It is important to understand the approximations and assumptions made in the PKS treatment,[21] since this was employed by Prassides and Day for the antimony halides. These are the following: (i) the two oxidation state subunits, Sb(III)/Sb(V) and Sb(V)/Sb(III), must have the same symmetry; (ii) the potential wells must be harmonic; (iii) each subunit has just one totally symmetric, normal mode; and (iv) both oxidation states have equal force constants (equal potential well curvatures). For the case of Sb(III)/Sb(V) with its superlattice of $SbCl_6^{3-}$ and $SbCl_6^-$ units, the predictions using these approximations and assumptions lead to reasonable agreement with the experimental data.

In Figure 6, we present an analogous potential energy diagram to assign and interpret the experimental data observed for the mixed-valence ion **3**. However, the situation with respect to **3** appears to be somewhat more complex than that for the antimony and platinum halides. Although **3a** and **3b** seem reasonable structures for describing the ground states of **3**, we have no rigorous proof for the geometry of these assignments. In fact, at present it is not possible to say with certainty whether or not **3** represents a so-called "unsymmetrical" case.[21]

Perhaps, this is best seen by examining structure **12**, a generalized presentation of the mixed-valence ion **3**. The single-crystal X-ray analysis of **8**[34] shows the distance between the ruthenium atoms and the planar benzene ring to be 1.75 Å, whereas the distance between the ruthenium atom and the planar butadiene fragment is 1.73 Å. Since **8** is a reasonable model for deducing the ruthenium–carbon ring separations in **12**, one would expect only a very small nuclear motion along the $Z$ axis of **12** during intervalence electron transfer. This is in contrast to the case of the antimony halides, where the nuclear motion during electron transfer is almost exclusively along an analogous $Z$ axis. Instead, viewing **12** as a composite of **3a** and **3b**, one would expect the major nuclear motion during electron transfer to be a Ru rocking motion along the $x$ axis. Spectroscopic studies, such as resonance Raman, or a crystal structure analysis of **3** would be helpful in this regard. Also, the role of the fluoroborate counterions and their nuclear motion during electron transfer are neglected with regard to Figure 6. Finally, several of the standard assumptions employed with the antimony and platinum halides[43,44] may not be valid for **3**.

Despite these drawbacks, though, Figure 6 is consistent with the experimental data for **3**. As shown in Figure 6, we know that there are two adjacent, and equal, potential wells, $Ru^0$–$Ru^{2+}$ and $Ru^{2+}$–$Ru^0$, separated by a barrier of $\Delta H^{\ddagger} = 12.7 \pm 0.8$ kcal/mol. If the *net* two-electron transfer in fact proceeds via two one-electron steps, then a $Ru^+$–$Ru^+$ potential well should touch the top of this barrier. Furthermore, $E_{op}$ is known to be 56.5 ± 0.3 kcal/mol. In essence, we know the four points shown by solid circles in Figure 6 and, by inference, the potential curves as well. Thus, despite differences noted previously, the type of diagram employed for the antimony and platinum halides appears to be quite reasonable to describe the properties of the mixed-valence ion **3**. Further study is needed regarding the validity and possible refinement of Figure 6, as well as its more general implications.

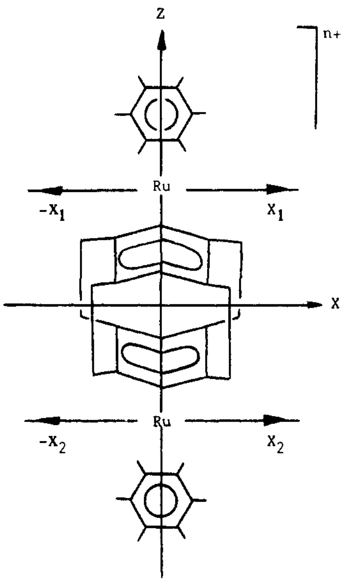

12

In summary, we have described the first example of a *net*, two-electron intervalence transfer of a discrete, mixed-valence organometallic complex. Values for $E_{th}$ and $E_{op}$ have been measured and used to construct a possible potential energy diagram for the mixed-valence ion **3**. The data are consistent with, but do not prove, a single-electron intervalence occurs to give the rate-determining transition state. The transfer of the second electron may then be of the type described by Richardson and Taube,[45] where it achieves considerable kinetic advantage by occurring within the ~$10^{11}$ s$^{-1}$ vibrational lifetime of the product derived from transfer of the first electron. These observations may well have general implication to the overall phenomenon commonly referred to as "concerted" multielectron transfers.[46]

## Experimental Section[47]

**Bis($\eta^6$-hexamethylbenzene)($\eta^6$,$\eta^6$-[2$_4$](1,2,4,5)cyclophane)diruthenium(II,II) Tetrakis(tetrafluoroborate) (2).** To 725 mg (1.08 mmol) of bis($\eta^6$-hexamethylbenzene)dichlorodi-$\mu$-chlorodiruthenium(II)[6] was added a solution of 850 mg (4.37 mmol) of silver tetrafluoroborate in 10 mL of acetone, and the mixture was stirred at room temperature for 30 min. After the precipitate was removed by filtration, the filtrate was concentrated to a volume of 2 mL. To this was added 61 mg (0.23 mmol) of [2$_4$](1,2,4,5)cyclophane followed by 10 mL of trifluoroacetic acid, and the mixture was boiled under reflux for 2 h. It was then cooled and the precipitate was collected by filtration. Solution of the precipitate in nitromethane followed by addition of anhydrous ether caused the separation of a yellow solid. This procedure of solution in nitromethane followed by addition of anhydrous ether was repeated twice more to give 215 mg (81%) of a pale yellow powder: mp 348–353 °C dec; $^1$H NMR ($CD_3NO_2$) $\delta$ 6.23 (4 H, s, Ar$H$), 3.8–3.1 (16 H, m, C$H_2$), 2.50 (36 H, s, C$H_3$).

---

(45) Richardson, D. E.; Taube, H. *Coord. Chem. Rev.* **1984**, *60*, 107–129 (see pp 125–127).

(46) We thank the referees who reviewed our manuscript for their insightful comments, which sharpened and improved our presentation.

(47) all NMR spectra were measured on a Nicolet 360 MHz instrument employing the computer program GNTXCH for simulating variable-temperature spectra. Visible spectra were obtained with a Beckman DU-7 spectrometer with the thermostat for the cell set at 30 ± 1 °C. The X-ray photoelectron spectral analyses were performed by Surface Laboratories, Inc. Melting points were taken with use of sealed, evacuated melting point capillaries and are uncorrected.

Anal. Calcd for $C_{44}H_{56}B_4F_{16}Ru_2 \cdot 3H_2O$: C, 44.47; H, 5.26. Found: C, 44.56; H, 5.08.

**Electrochemical properties of 2** were measured with use of an electrochemical station consisting of a Princeton Applied Research (PAR) Model 173 potentiostat/galvanostat driven by a PAR Model 175 universal programmer with a PAR Model 179 digital coulometer. Coulometry was carried out with a PAR Model 337 cell with a platinum mesh (22.8 $cm^2$) electrode. The cyclic voltammetry being reported was carried out at a scan rate of 100 mV/s with a 0.1 M solution of tetra-*n*-butylammonium tetrafluoroborate in an appropriate solvent. The three-electrode cell contained a spherical platinum working electrode, a platinum wire counterelectrode placed coaxial to the working electrode, and a silver chloride coated, silver wire quasireference electrode isolated from the bulk solution by a single-fritted compartment. After the completion of each experiment, ferrocene was added and the cyclic voltammogram was repeated so that the ferrocene redox potential provided a reference for converting measured redox potentials to approximate standard calomel electrode (SCE) values (ferrocene/ferrocinium in acetone, $E_{1/2} = +0.500 \pm 0.005$ vs. SCE).

The cyclic voltammogram of **2** was measured in acetone at room temperature, and as presented in Figure 1, it shows two reversible, two-electron waves: $E_{1/2}(\text{SCE}) = -0.060 \pm 0.005$ V, $\Delta E_p = 35 \pm 3$ mV, $i_a/i_c = 1.00 \pm 0.01$; $E_{1/2}'(\text{SCE}) = -0.593 \pm 0.005$ V, $\Delta E_p = 36 \pm 3$ mV, $i_a/i_c = 0.95 \pm 0.05$. The $\Delta E_p$ values indicated that each wave corresponded to a two-electron transfer, and this was confirmed by coulometry. The cyclic voltammogram of **2** was also measured in other solvents such as dichloromethane and propylene carbonate, but the voltammogram in acetone showed the highest chemical reversibility.

**Bis($\eta^6$-hexamethylbenzene)($\eta^4$,$\eta^4$-[$2_4$](1,2,4,5)cyclophane)diruthenium(0,0) (4). (A) By Bulk Electrolysis of 2.** Bulk electrolytic reduction of **2** was conducted in an inert atmosphere box with a modified H-cell. To each compartment of the electrolysis cell was added a 0.1 M solution of tetra-*n*-butylammonium hexafluorophosphate in acetone. A background cyclic voltammogram was then taken to establish that no electroactive species were present. After addition of 147 mg (0.13 mmol) of **2** to the right-hand compartment of the cell with stirring to effect solution, a second voltammogram was taken in the range of 0.0 to −2.0 V. On the basis of the observed reduction potentials, the potential for the bulk electrolysis was set at a value 100 mV more negative than the second reduction potential ($E_{1/2}'$). A carbon cloth electrode was connected and electrochemical reduction of **2** was initiated with stirring. The uptake of electrons was monitored with a PAR Model 179 Digital Coulometer and, after four electron-equivalents had passed, the reduction was stopped. The course of the reduction could also be followed by eye. At the start the solution is pale yellow, it becomes dark red during formation of **3**, and finally it becomes a golden yellow with the formation of **4**.

The resulting product is only slightly soluble in acetone; therefore, most of the compound was adsorbed on the carbon electrode. The electrode was extracted four times with 25-mL portions of benzene, and the combined benzene extracts were concentrated under reduced pressure. The remaining golden yellow acetone solution was also evaporated to dryness, and the rest of the reduced product was extracted with benzene. The crude product was then washed with 5 mL of acetone to dissolve any remaining electrolyte. To remove side products, the residual solid was also washed with 5 mL of hexane. To remove pieces of carbon cloth that had separated from the electrode and were present in the residual solid, the product was redissolved in benzene and filtered, and the benzene filtrate was concentrated. This gave 94 mg (92%) of a yellow powder: mp >290 °C dec; $^1$H NMR ($C_6D_6$) $\delta$ 2.63–1.75 (16 H, m, C*H*$_2$), 1.96 (4 H, s, Ar*H*), 1.92 (36 H, s, C*H*$_3$); mass spectrum, *m/e* 779, 780, 781, 782, 783, 784, 785, 786, 787, 788, 789, 790, 791, 792, 793 (a computer simulation reproduced this expected isotope distribution pattern precisely with respect to both signal and intensity).

Anal. Calcd for $C_{44}H_{56}Ru_2$: C, 67.10; H, 7.20. Found: C, 66.80; H, 7.10.

**(B) By Chemical ("Electron Reservoir") Reduction of 2.** A mixture of 36 mg (0.003 mmol) of **2** and 27 mg (0.06 mmol) of bis(hexamethylbenzene)ruthenium(0), **8**,[36] in 15 mL of dry, degassed methanol was stirred at room temperature for 4 h in an inert atmosphere box. The course of the reduction could be followed by eye. At the start the solution was colorless (both starting materials, **2** and **8**, are insoluble), it became a dark, reddish purple after 5 min of stirring, and then it finally became yellow with the formation of **4**. The reaction mixture was concentrated, and the residue was extracted with three 7-mL portions of benzene. After removal of the insoluble byproduct, bis($\eta^6$-hexamethylbenzene)ruthenium(II) tetrafluoroborate, by filtration, the combined benzene extracts and filtrate were concentrated. The resulting yellow solid was washed first with three 5-mL portions of hexane and then with two 3-mL portions of tetrahydrofuran to give 22 mg (88%) of a yellow powder identical in all respects with that obtained by procedure A.

Table I. Variable-Temperature $^1$H NMR Data for **3**

| *T*, K | $\tau$, s | log (*k*/*T*) (range) |
|---|---|---|
| 273 | $3.0 \pm 0.1 \times 10^{-5}$ | 2.09 (2.10–2.07) |
| 253 | $3.8 \pm 0.2 \times 10^{-4}$ | 1.02 (1.04–1.00) |
| 243 | $9.0 \pm 0.2 \times 10^{-4}$ | 0.66 (0.67–0.65) |
| 233 | $2.8 \pm 0.2 \times 10^{-3}$ | 0.19 (0.22–0.16) |
| 228 | $3.9 \pm 0.2 \times 10^{-3}$ | 0.05 (0.08–0.03) |
| 223 | $6.6 \pm 0.3 \times 10^{-3}$ | −0.17 (−0.15–(−0.19)) |
| 213 | $3.0 \pm 0.3 \times 10^{-2}$ | −0.80 (−0.75–(−0.84)) |
| 193 | $1.0 \pm 0.5$ | −2.29 (−1.99–(−2.46)) |

The reduction of **2** to **4** could also be carried out with a 2% sodium amalgam in 1,2-dimethoxyethane. An identical product was again obtained, but the yield in this case was only 34%.

**(C) By Chemical (Electron Reservoir) Reduction of 3.** To a solution of 21 mg (0.02 mmol) of **3** in 10 mL of dry, degassed methanol was added with stirring 9 mg (0.02 mmol) of **8**[36] in an inert atmosphere box. After the mixture had been stirred for 4 h, it was worked up in the same manner previously described in procedure B to give 16 mg (93%) of a yellow powder, identical in all respects with the samples of **4** obtained by procedures A and B.

**Bis($\eta^6$-hexamethylbenzene)($\eta^4$,$\eta^6$-[$2_4$](1,2,4,5)cyclophane)diruthenium(0,II) Bis(tetrafluoroborate) (3). (A) By Reaction of 2 and 4.** A mixture of 15 mg (0.013 mmol) of **2** and 10 mg (0.013 mmol) of **4** in 15 mL of dry, degassed methanol was stirred for 1 h at room temperature in an inert atmosphere box. The resulting dark, purplish-red solution was concentrated to give 25 mg (100%) of **3** as a dark, purplish-red solid. This was recrystallized from dichloromethane to give long, thin purplish-red needles having a metallic sheen. A sample recrystallized from methanol gave dark red needles: mp >337 °C dec; $^1$H NMR ($CD_2Cl_2$ at 25 °C) $\delta$ 2.55–1.80 (16 H, m, C*H*$_2$, overlapping 4 H, s, Ar*H*), 2.17 (36 H, C*H*$_3$); $^1$H NMR ($CD_2Cl_2$ at −80 °C) $\delta$ 2.55–1.45 (16 H, m, C*H*$_2$, overlapping 2 H, s, Ru$^{II}$–Ar*H*, and 2 H, s, Ru$^0$–Ar*H*), 2.36 (18 H, s, Ru$^{II}$–C*H*$_3$), 1.87 (18 H, s, Ru$^0$–C*H*$_3$); $^{13}$C NMR ($CD_2Cl_2$ at 25 °C, proton decoupled and with partial proton coupling to indicate spin multiplicity) $\delta$ 17.4 (q, Ar–*C*H$_3$), 28.2 (t, *C*H$_2$), 77.2 (d, cyclophane–Ar–*C*H), 100.2 (s, Ar–*C*–CH$_3$, overlapping s, cyclophane–Ar*C*–CH$_2$). At −60 °C, the $^{13}$C NMR signal at $\delta$ 17.4 splits into two signals at $\delta$ 17.1 and 17.7.

Anal. Calcd for $C_{44}H_{56}Ru_2B_2F_8$: C, 55.01; H, 5.88. Found: C, 54.60; H, 5.55.

**(B) By Chemical (Electron Reservoir) Reduction of 2.** A mixture of 43 mg (0.004 mmol) of **2** and 17 mg (0.04 mmol) of bis(hexamethylbenzene)ruthenium(0), **8**,[36] in 15 mL of dry, degassed methanol was stirred at room temperature for 1 h in an inert atmosphere box. The resulting dark purplish-red solution was concentrated, and the residue was extracted with three 5-mL aliquots of degassed dichloromethane. Filtration of the dichloromethane extracts followed by concentration gave 37 mg (100%) of dark, purplish-red crystals, identical in all respects with the sample from procedure A. Method B is clearly the preferable choice for preparing **3**.

**A variable-temperature $^1$H NMR study** of **3** was made with $CD_2Cl_2$ as solvent, as shown in Figure 2. The signal, whose coalescence and splitting was observed, is that of the methyl protons present in the two hexamethylbenzene decks. The spectra were taken at eight different temperatures, ranging from 0 to −80 °C. Alongside these spectra in Figure 2 are computer simulations deduced by using the GNTXCH two-site program of the Nicolet 360-MHz spectrometer. The coalescent temperature was found to be −43 °C. In Table I are listed the temperatures (*T*) for each measurement, the computer-determined mean lifetime of the nucleus in each site ($\tau$), and the corresponding values of log (*k*/*T*), where *k* is the reciprocal of $\tau$.

From these data the rate process was analyzed with use of the Eyring equation. The plot of log (*k*/*T*) vs. 1/*T* is given in Figure 3. From a linear regression calculation the correlation coefficient for the line drawn in Figure 3 is 0.997. The values of the activation parameters for the dynamic equilibrium of **3a** ⇌ **3b** were found to be $\Delta H^{\ddagger} = 12.7 \pm 0.08$ kcal/mol; $\Delta S^{\ddagger} = 8 \pm 3$ cal/(mol K); and $\Delta G^{\ddagger}$(at 25 °C) = $10.3 \pm 0.8$ kcal/mol.

**Electronic absorption spectral studies of 3** were made on a Beckman DU-7 spectrometer, and the absorption spectrum for **3** in dichloromethane is shown in Figure 5. The values found for the apparent Gaussian-shaped absorption band are $\lambda_{max}$ 506.0 nm ($\nu_{max}$ 19 800 ± 100 $cm^{-1}$), $\epsilon$ 485 ± 27 $M^{-1}$ $cm^{-1}$, and $\Delta\nu_{1/2}$ 9000 ± 200 $cm^{-1}$. As would be expected, the absorption band is affected by changing the polarity of the solvent. Thus, with acetonitrile as solvent, the values are $\lambda_{max}$ 487.0 ($\nu_{max}$ 20 500 ± 100 $cm^{-1}$), $\epsilon$ 739 ± 48 $M^{-1}$ $cm^{-1}$, and $\Delta\nu_{1/2}$ 9800 ± 200 $cm^{-1}$; whereas with methanol as solvent, these values are $\lambda_{max}$ 484.5 ($\nu_{max}$ 20 600 ± 100 $cm^{-1}$), $\epsilon$ 922 ± 53 $M^{-1}$ $cm^{-1}$, and $\Delta\nu_{1/2}$ 9300 ± 200 $cm^{-1}$. On the basis of the dielectric continuum model, a plot of $\lambda_{max}$ of the intervalence transfer band in different solvents vs. $(1/D_{op} - 1/D_s)$ can be used to obtain values for the solvent reorganizational energy and the internal reorganizational energy for electron transfer.[18,19] The data above provide three points for such a plot for **3**. Unfortunately, attempts to make additional measurements of **3** with other suitable solvents were not successful, primarily due to dissociation of the complex **3** in these other solvents. In our opinion three points are not adequate for making such a plot, and so we have not made an analysis of this type.

Compounds **2** and **4** show only end absorption, beginning strongly at 380 nm and tailing off into the visible but with very weak absorption above 440 nm. Thus, the chromophores present in **2** and **4** have essentially no effect with respect to the absorption band presented in Figure 5. The absorption spectra of solutions of **3**, both in acetone and in dichloromethane, were measured through the range of 800 to 1900 nm on a Perkin Elmer Coleman EPS-3T instrument. No absorption was detected other than a small amount of tailing at 800 nm from the absorption band shown in Figure 5.

**Acknowledgment.** We thank the National Science Foundation for their support under Grants CHE-8400421 (V.B.) and CHE-8313459 (R.G.F.). We also thank the National Institutes of Health (RR02336) and the National Science Foundation (CHE-8411177) for funds making possible the purchase of the General Electric QE 300-MHz spectrometer used in this study. R.G.F. thanks the Dreyfus (1982–1987) and Guggenheim (1984–1986) Foundations for Fellowships.

**Registry No. 2**, 82871-70-3; **3**, 104350-57-4; **4**, 104335-71-9; **8**, 32732-05-1; bis($\eta^6$-hexamethylbenzene)dichloro-di-$\mu$-chlorodiruthenium(II), 67421-02-7; $[2_4]$(1,2,4,5)cyclophane, 54100-59-3.

---

# Carbon Acidity. 71. The Indicator Scale of Lithium Ion Pairs in Tetrahydrofuran

**Scott Gronert and Andrew Streitwieser, Jr.***

*Contribution from the Department of Chemistry, University of California, Berkeley, California 94720.* *Received June 3, 1986*

**Abstract:** An equilibrium lithium ion pair indicator scale has been established for eight hydrocarbons that form solvent-separated ion pairs in THF. The scale covers the p$K_a$ range from 18.49 to 23.84 relative to 9-phenylfluorene at p$K_a$ = 18.49. This range allows the study of enolates and other highly stabilized anions under realistic synthetic reaction conditions. Equilibria were monitored with UV–vis spectroscopy, and the indicator anion spectra are reported. Thermodynamic measurements of the indicator equilibria yield small $\Delta S^\circ$ values indicating that all of the solvent-separated ion pairs must have similar structures and solvation. Comparison of these thermodynamic parameters with those measured for the analogous cesium ion pairs points out the more complex nature of organocesium ion pairing. Aggregation studies indicate that the organolithium salts exist predominantly, if not exclusively, as monomers in the concentration range employed ($10^{-3}$–$10^{-4}$ M).

One of the most important reaction sequences in modern synthetic organic chemistry is metalation with lithium amide or an alkyllithium, usually the commerically available butyllithium, in an ether solvent followed by treatment with an electrophilic reagent.[1] The metalation process is usually kinetically controlled although thermodynamic acidities play an important role. Careful control of reaction conditions and sequences are important for directing regio- and stereoselectivity in these syntheses. Consequently, there has been recent intense interest in the structures, stabilities, and reactivities of ion pair salts of carbanions, especially with lithium as the gegenion.[2,3]

A lithium ion pair carbon acidity scale in THF, a solvent frequently used in metalation sequences, would clearly be of enormous use in synthetic design. The establishment of such a scale, however, is complicated by the complex nature of lithium ion pairs. Lithium salts of carbanions in ethers are known to form contact and solvent-separated ion pair structures to varying degrees as well as aggregates.[4-16] Accordingly, our first research in this direction established a carbanion indicator scale in THF with cesium as the gegenion.[17] Cesium salts of carbanions generally form contact ion pairs that we considered would provide a simpler reference system. Related carbon acidity scales have been es-

---

(1) (a) Stowell, J. C. *Carbanions in Organic Synthesis*; Wiley: New York, 1979. (b) Augustine, R. L. *Carbon–Carbon Bond Formation*; Dekker: New York, 1979. (c) Eliel, E. L.; Otsuka, S. *Asymmetric Reactions and Processes in Chemistry*; American Chemical Society: Washington, 1982. (d) House, H. O. *Modern Synthetic Reactions*; Benjamin/Cummings: Menlo Park, 1972.

(2) (a) Buncel, E.; Durst, T. *Comprehensive Carbanion Chemistry: Part A*; Elsevier: New York, 1980. (b) Buncel, E.; Durst, T. *Comprehensive Carbanion Chemistry: Part B*; Elsevier: New York, 1984.

(3) Coetzee, J. F.; Ritchie, C. D. *Solute-Solvent Interactions*; Dekker: New York, 1969.

(4) Smid, J. In *Ions and Ion Pairs in Organic Reactions*; Szwarc, M., Ed.; Wiley: New York.

(5) Hogen-Esch, T. E.; Smid, J. *J. Am. Chem. Soc.* **1966**, *88*, 307.

(6) (a) Grutzner, J. B.; Lawlor, J. M.; Jackman, L. M. *J. Am. Chem. Soc.* **1972**, *94*, 2306. (b) O'Brien, D. H.; Russell, C. R.; Hart, A. J. *J. Am. Chem. Soc.* **1979**, *101*, 633. (c) Menon, B.; Buncel, E. *J. Organomet. Chem.* **1978**, *159*, 357. (d) Buncel, E.; Menon, B. C.; Colpa, J. P. *Can. J. Chem.* **1979**, *57*, 999. (e) Fraenkel, G.; Geckle, M. J.; Kaylo, A.; Estes, D. W. *J. Organomet. Chem.* **1980**, *197*, 249. (f) Parkes, H. M.; Young, R. N. *J. Chem. Soc., Perkin Trans. 2* **1980**, 1137. (g) Chan, L. L.; Smid, J. *J. Am. Chem. Soc.* **1968**, *90*, 4654. (h) Bushby, R. J.; Patterson, A. S. *J. Chem. Res. Synop.* **1980**, 306. (i) Edlund, U. *Org. Magn. Reson.* **1979**, *12*, 661.

(7) Velthorst, N. H. *Pure Appl. Chem.* **1979**, *51*, 85.

(8) (a) Wiedrich, C. R.; Catlett, D. L., Jr.; Sedgwick, J. B.; Stevenson, G. R. *J. Phys. Chem.* **1983**, *87*, 578. (b) Müllen, K.; Huber, W.; Meul, T.; Nakagawa, M.; Iyoda, M. *Tetrahedron* **1983**, *39*, 1575. (c) Young, R. N. *Prog. Nucl. Magn. Reson. Spectrosc.* **1979**, *12*.

(9) (a) Hogen-Esch, T. E.; Smid, J. *J. Am. Chem. Soc.* **1966**, *88*, 318. (b) Smid, J. *Angew. Chem., Int. Ed. Engl.* **1972**, *11*, 112.

(10) (a) McGarrity, J. F.; Ogle, C. A. *J. Am. Chem. Soc.* **1985**, *107*, 1805. (b) Holm, T. *Acta Chem. Scand., Ser. B* **1978**, *32*, 162.

(11) Bauer, W.; Seebach, D. *Helv. Chim. Acta* **1984**, *67*, 1972.

(12) (a) West, P.; Waack, R.; Purmont, J. I. *J. Am. Chem. Soc.* **1970**, *92*, 840. Waack, R.; Doran, M. A. *J. Am. Chem. Soc.* **1969**, *91*, 2456. (c) West, P.; Waack, R. *J. Am. Chem. Soc.* **1967**, *89*, 4395.

(13) Exner, M. M.; Waack, R.; Steiner, E. C. *J. Am. Chem. Soc.* **1973**, *95*, 7009.

(14) Hogen-Esch, T. E.; Smid, J. *J. Am. Chem. Soc.* **1967**, *89*, 2764.

(15) Hassig, R.; Seebach, D. *Helv. Chim. Acta* **1983**, *66*, 2269.

(16) Takai, U.; Hogen-Esch, T. E.; Smid, J. *J. Phys. Chem.* **1972**, *76*, 2152.

(17) Bors, D. A.; Kaufman, M. J.; Streitwieser, A., Jr. *J. Am. Chem. Soc.* **1985**, *107*, 6975.

0002-7863/86/1508-7016$01.50/0